Journal of
Ship&Ocean
Technology
©MARCH 2006

SOTECH Vol. 10, No. 1, pp. 27 ~ 37, 2006

Estimation of Current Loads on Offshore Vessels Using CFD

Rae-Hyung Yuck[1], Hang-Soon Choi[1] and Sa-Young Hong[2]

[1] Seoul National University, Seoul, Korea; E-mail: fstars@nownuri.net
[2] Maritime and Ocean Engineering Research Institute, Daejeon, Korea; E-mail: sayhong@moeri.re.kr

Abstract

Current loads acting on offshore vessels are important for predicting the hydrodynamic and structural responses of the vessels. It is also true for analyzing the behavior of moored systems under the action of ocean current. Unfortunately there are few standardized current load coefficients for offshore vessels and it is extremely difficult to be applied to arbitrary hull shapes, if any. Therefore current load coefficients for three hull shapes are calculated in this study using a CFD code, which is well known in the shipbuilding industry. In order to validate the present approach, a typical VLCC is taken as numerical example and resulting current coefficients are compared with experiment together with the OCIMF data. The comparison shows a good agreement in the qualitative sense. Two additional models considered herein are a shuttle tanker and a FPSO under deepwater condition ($WD/T \geq 6$). The present numerical approach may be utilized for practical design of offshore vessels.

Keywords: current force coefficient, offshore vessels, FPSO, VLCC, Fluent, hybrid mesh

1 Introduction

Environmental loads due to wind, current and wave must be considered in analyzing the motion of offshore vessels in order to examine the watch circle and ensure its operability. Among various environmental load types, current and wind loads are normally assessed empirically because these are caused by fluid viscosity and thus it is difficult to estimate them theoretically. Moreover, there are few standardized load coefficients for offshore vessels. In practice, wind and current loads on offshore vessels are usually estimated with the help of OCIMF's (Oil Companies International Marine Forum) experimental data published in 1977 and revised in 1994. OCIMF carried out towed tests extensively for VLCCs and they compiled experimental data into the current load coefficient statistically. However, it is not clear whether the OCIMF data can be applied o arbitrary hull shapes.

In order to estimate current and wind loads on offshore structures accurately, towing and wind tunnel tests must be carried out. But, this is not always recommendable because of the need for experimental facilities, the huge cost and long time consumption, besides the inherent scale-effect problem. With keeping the fact in mind, we present a numerical method for predicting the current force acting on various hull shapes. A viscous flow code which is well known in the field of naval architecture is used.

First, we calculate a typical VLCC(hereafter referred to as KVLCC) for comparing with the OCIMF data and also with experimental data. Two additional models considered in this study are a shuttle tanker, which is basically of the same configuration as KVLCC, and a FPSO.

2 Flow Analysis

2.1 A Viscous Code

A viscous code known as FLUENT is used herein. This code adopts the finite volume method, which integrates the governing equation in a small discrete region of the flow domain. This method satisfies the continuity of fluid automatically and fits any kind of grid systems to a certain extent.

For steady flow, the convection term can be discretized by the second-order upwind method, whereas the pressure gradient term by the standard method. SIMPLEC is adopted for the velocity-pressure coupling terms. It was proved that these methods can provide the exact solution for the viscous flow near hull(Yun et al 2001).

As it is already well known, the turbulence modeling is the most important part for calculating viscous flow near the streamlined body like a ship, because it affects the accuracy of the solution strongly(Larsson et al 2000). In this work, the two equation standard $k-\varepsilon$ model is taken, and Reynolds stress transport model is also applied partially. The standard wall function is used, which may compensate the accuracy to some extent, when grids near the body are not enough dense(Kim et al 2000, 2002).

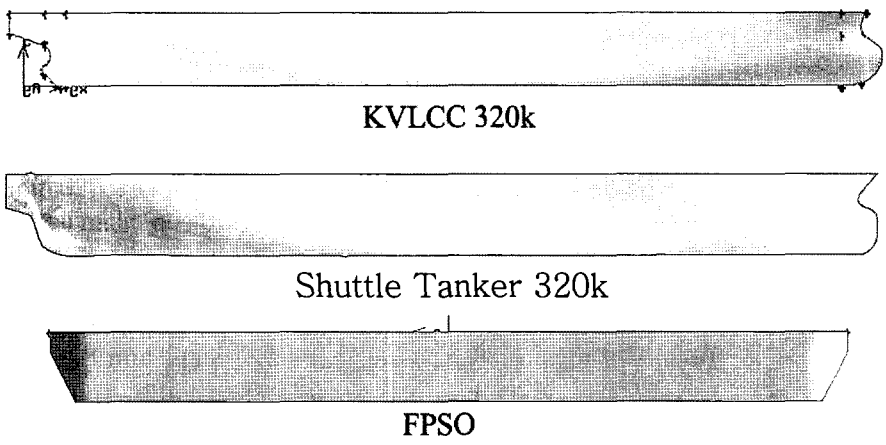

Fig. 1 Profile of Calculation Models

As it is already known, the accuracy of the solution is depended on the kind of grid system used and the turbulence model yields different flow characteristics depending on that grid system. In general, hexahedral mesh and the hybrid mesh (hexahedral + tetrahedral) we used herein, is known to yield good results for the turbulence model with the wall function. In this work, the flow direction varies in each case depending on the current angle of attack, thereby causing a complex geometry with respect to inflow with

high Reynolds number (about $10^{6\sim8}$). We found that the tetrahedral mesh is appropriate when the flow is not aligned with the grid (Ito 2002, Fluent user's guide 1998).

2.2 Model

Models are shown in Fig. 1 and the particulars of the models are listed in Table 1. KVLCC 300k is taken as a bench-mark test for comparing with experiment and the OCIMF data. A shuttle tanker, which is bulkier than KVLCC and deeper in draft, is also considered. Lastly a FPSO, which looks like a box and symmetric fore and aft, is taken. The geometric characteristics of KVLCC, shuttle tanker and OCIMF's model are summarized in Table 2. The purpose of this comparison is to examine the dependence of the current load on the hull shape.

2.3 Mesh Generation

Flows inside the boundary layer must be captured rightly when we want to estimate the viscous force correctly. In addition to the suitable discretization and turbulence model, high resolution grids near the body must be provided. In this study, rectangular cells of approximately ten thousands are generated on the body surface and hexahedral cells are laid above the surface meshes, while the outer domain is discretized with tetrahedral meshes. This grid system makes it possible to calculate the current force encountered by various directional inflows within high Reynolds regions using one domain. As shown in Fig. 2, the computation domain is divided into about 450,000 cells concentrated near the body. Outer boundary condition is also depicted in this figure.

Table 1 Main Dimensions of Computation Models

	Lbp(m)	Breadth(m)	Draft(m)
KVLCC	320	58	20.8
VLCC	320	60	25
FPSO	285	63	24.45

Table 2 Geometric Characteristics of Computation Models

	KVLCC	Shuttle	OCIMF
Lbp/Breadth	5.51	5.33	6.3-6.5
Breadth/Draft	2.78	2.4	2.2-2.6
r/Breadth	0.01	0.01	0-0.07

*r is bilge radius.

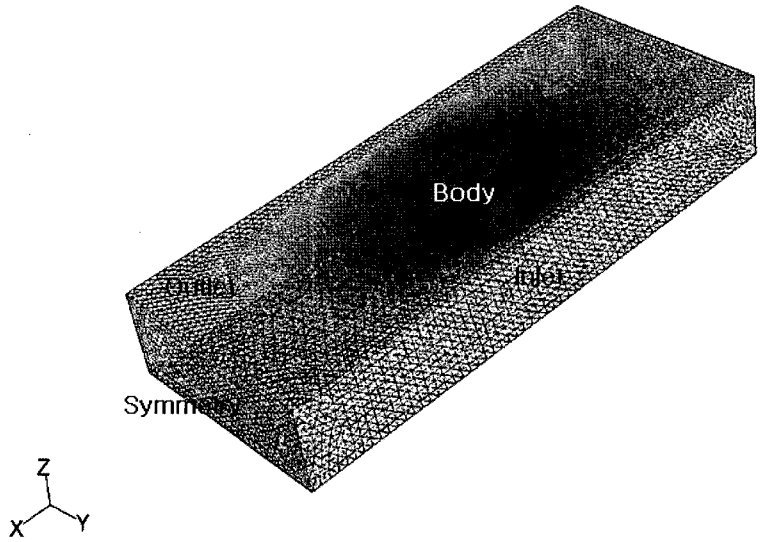

Fig. 2 Grid System

3 Results and Discussion

3.1 Computation

All calculations are made under deepwater condition ($WD/T \geq 6$), but without considering the free surface. The current speed is taken as 1m/s and the current direction changes from the head sea (180°) to the following sea (0°) with an interval of 10 degrees. The boundary condition of the domain is set up depending on the current direction. The convergence criteria of the solution may be determined by searching the scaled-residual of flow velocities, k and ε. The scaled-residual, SR is defined by Eq.

$$SR = \frac{R^{\phi}_{iteration\ N}}{R^{\phi}_{iteration\ 5}}$$

$$\text{with, } R^{\phi} = \sum_{cellP} \left| \sum_{nb} a_{nb}\phi_{nb} + b - a_P\phi_P \right|$$

Where ϕ_P is a general variable ϕ at a cell P and a_{nb} is the influence coefficients for the neighboring cells and a_P is the center coefficient and b is the contribution of the constant part of the source term. The denominator of Eq. is the largest absolute value of the residual during the first five iterations. The convergence criterion requires that the scaled-residual decrease to 10^{-3} for all cases. Convergence time ranges from an hour to several hours for Pentium-IV 2GHz processor depending on the current direction. The computation time is relatively short for the mesh size. This is one of the merits for the calculation code we used.

3.2 Simulation

Velocity and pressure contours are illustrated in Figs. 3. We can see that for the head current, the flow field is not disturbed much as expected. But the flow pattern for the beam current appears to be much more complex and even vortex shedding can be observed. In this case, the calculation time is much longer than that needed for the head current because of the convergence rate.

3.3 Current Force Coefficient

The current force can be expressed in the form given by Eq. 1. This equation uses the same notations and normalizing parameters as used in the OCIMF data.

$$F_{Xc} = \frac{1}{2} C_{Xc} \rho_c V_c^2 L_{BP} T$$
$$F_{Yc} = \frac{1}{2} C_{Yc} \rho_c V^2 L_{BP} T \qquad (1)$$
$$M_{XYc} = \frac{1}{2} C_{XYc} \rho_c V_c^2 L_{BP}^2 T$$

where C_{Xc}, C_{Yc}, C_{XYc} are the longitudinal current force coefficient, lateral current force coefficient and current yaw moment coefficient in this order.

The current force coefficients for KVLCC are depicted in Figs. 4~6. Towing tests for the scaled model of KVLCC with 1:160 were carried out in order to validate our numerical method in the towing tank at a low speed of 0.3 m/s. The longitudinal coefficient compares well with experimental ones, but some discrepancies are observed in the cases near the beam current. The discrepancies may be caused by the instability of turbulent kinetic properties in the inlet boundary due to the short distance between the current inlet and the body. But the yaw moment coefficient compares well with experimental data near the beam current condition. The yaw moment is the result of turning forces about the mid-ship. Therefore the yaw moment may be predicted well even though the entire forces acting on the hull surface are unstable. The different result for KVLCC and OCIMF's model seems to be caused by the difference in geometry. It means that if the geometric characteristic (Table 2) is different, vessels of the same kind could have different current coefficients. If it is true, we may conclude that the current load on vessels is very sensitive to its hull shape and we should be careful to estimate the current load on a vessel using published data.

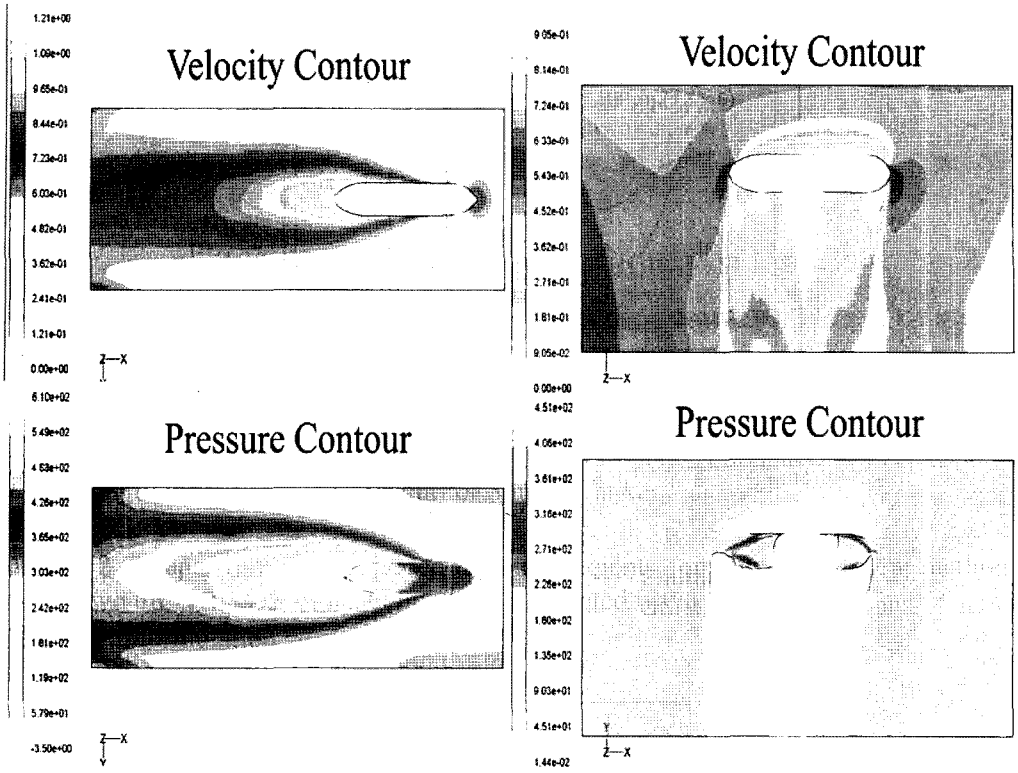

(a) Head Current (b) Beam Current

Fig. 3 Velocity and Pressure Contour for Head/Beam Current Condition

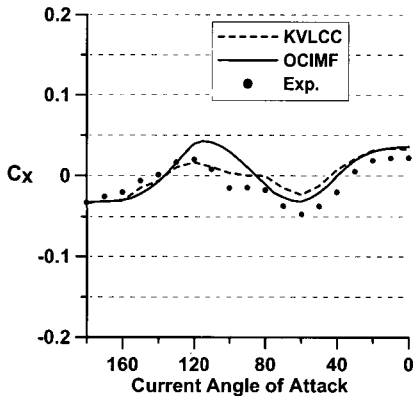

Fig. 4 Comparison between Calculation and Experiment for Longitudinal Force Coefficient for KVLCC

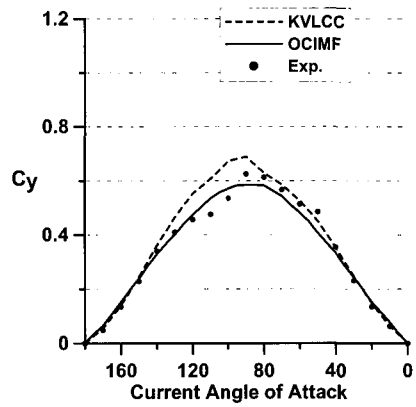

Fig. 5 Comparison between Calculation and Experiment for Lateral Force Coefficient for KVLCC

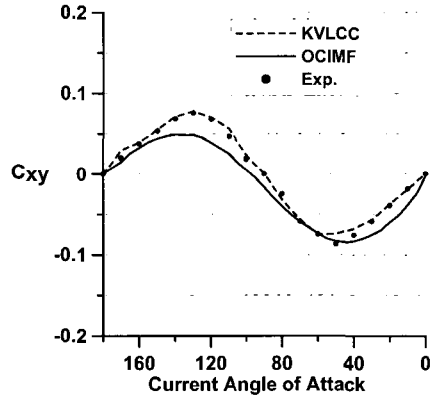

Fig. 6 Comparison between Calculation and Experiment for Yaw Moment Coefficient for KVLCC

Results for the shuttle tanker are shown in Figs. 7~9. It can be seen in Fig. 7 that the longitudinal coefficient is much lager than OCIMF's data. It is believed that the viscous drag increases due to the deeper draft. In Fig. 8, it is observed that the lateral coefficient also increases near the beam current. It may be conjectured that increased lateral current force is attributed mainly to the bluffer hull shape of the KVLCC and shuttle tanker (larger breadth than OCIMF's model as shown in Table 2). It is to note that the lateral force coefficient near the beam current becomes much lager as the value of Lbp/B decreases. The current angle, at which the yaw moment becomes zero, shifts towards backward because the measuring point of the yaw moment differs from the midship, which is the center of the yaw moment in the case of OCIMF's model.

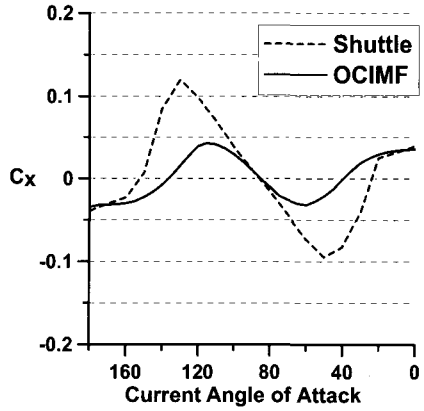

Fig. 7 Comparison between Calculation and Published Data for Longitudinal Force Coefficient for Shuttle Tanker

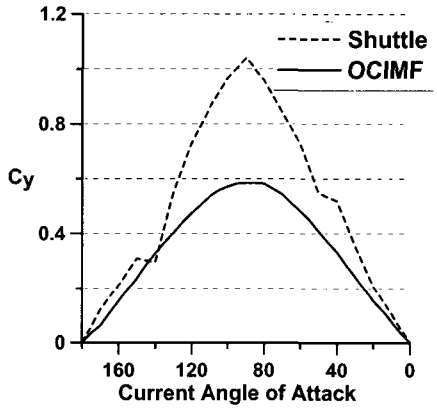

Fig. 8 Comparison between Calculation and Published Data for Lateral Force Coefficient for Shuttle Tanker

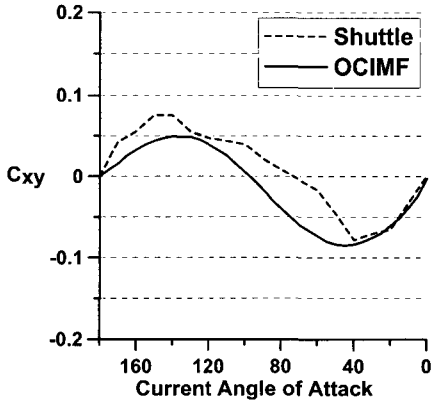

Fig. 9 Comparison between Calculation and Published Data for Yaw Moment Coefficient for Shuttle Tanker

Numerical results of FPSO are depicted in Figs.10~12 together with the previous ones. The current force coefficient of FPSO shows a slightly different pattern. Especially, the longitudinal coefficient has the opposite sign to that of VLCCs in the range from 100° to 160°. This means that FPSO is continuously drifted away by the current because FPSO is almost like a box. Vessels of this configuration does not experience opposite forces against the current. The lateral and moment coefficients are similar to those of KVLCC, but the magnitude is a little bit different because of the hull shape.

It is intended in this study to examine the possibility of estimating current forces on vessels with arbitrary shape using a viscous code and to provide design data for offshore operations. Based on the computational results, we may conclude that the present numerical approach can be used for practical applications. Towing tests for the shuttle and FPSO must be carried out in order to validate the calculation results, particularly free surface effect and further studies for multiple vessels will be done in the near future.

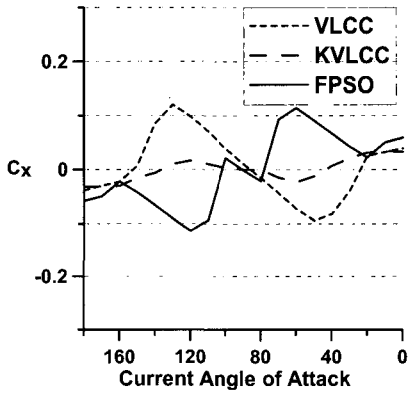

Fig. 10 Comparison between Three Models for Longitudinal Force Coefficient for FPSO

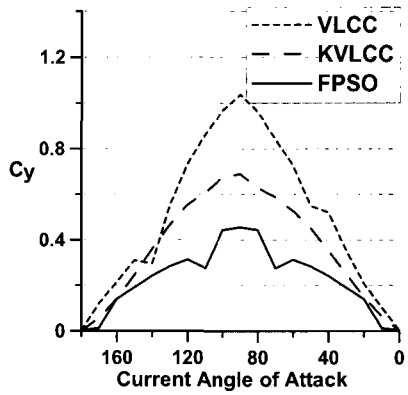

Fig. 11 Comparison between Three Models for Lateral Force Coefficient for FPSO

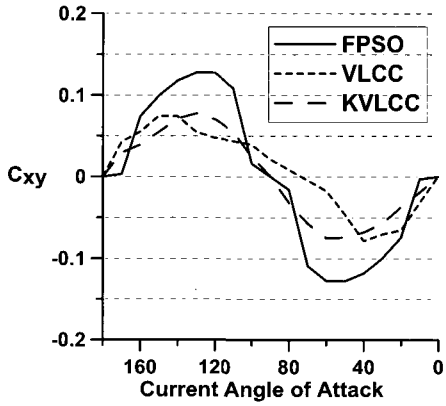

Fig. 12 Comparison between Three Models for Yaw Moment Coefficient for FPSO

4 Conclusions

A numerical approach has been proposed to estimate the current load on offshore structures using a CFD code, FLUENT. Three types of models are considered. The numerical result for KVLCC model shows good agreement with the experimental data. Based on it, it may be concluded that a viscous code like FLUENT can be applied to predict the current force on offshore vessels for practical uses. The shuttle tanker and FPSO show a clear discrepancy from the OCIMF's data. This may be due to the different shape, which indicates that the current force is very sensitive to the hull shape. From these computations, we can conclude that special concerns are needed when the empirical current coefficient is applied. Lastly it is pointed that further validation is needed by towing tank experiment.

Acknowledgement

The authors would like to thank the financial support of Korea Research Institute of Ship and Ocean Engineering (recently changed by Maritime and Ocean Engineering Research Institute) for this work.

References

Fluent5 User's Guide. 1998. Fluent Incorporated.

Fluent5 Tutorial Guide. 1998. Fluent Incorporated.

Ito Y. and N. Kazuhiro. 2002. Unstructured Mesh Generation for Viscous Flow Computations. Proc of 11th International Meshing Roundtable, New York, pp 367-378.

Kim W.-J., D.-H. Kim and S.-H. Van. 2000. A Study on the Turbulence Flow Calculation near the Merchant Ship using the Finite Volume Method, Journal of the Society of Naval Architects of Korea, Vol 37, No 4, pp 19-30.

Kim W.-J., D.-H. Kim and S.-H. Van. 2002. Computational Study on the Turbulence Flows around Modern Tanker Hull Forms. Int. J of Numerical Methods in Fluids, Vol 38, No 4, pp 377-406.

Larsson L., F. Stern, V. Bertram. 2000. Gothenburg 2000. A Work Shop on Numerical Ship Hydrodynamics, Gothenburg, Sweden.

Prediction of Wind and Current Loads on VLCCs(2nd edition). 1994. Oil Companies International Marine Forum.

Wurtzler K.-E., R.-F. Tomaro and F.-C. Witzeman. 2000. Analysis of Three Unstructured Grid Techniques From a User's Perspective. Proc of the 7th International Conference on Numerical Grid Generation in Computational Field Simulation, Whistler, pp 357-366.

Yun J.-D., M.-C. Ryu and Y.-S. Kim. 2001. Calculations of Viscous Flow Field near the Hull using a Commercial CFD Program, Fluent, Proc of the Society of Naval Architects of Korea, Seoul, pp 279-283.